

Human Multicomponent Micro-Doppler Signals Separation Based on a Novel Local Time-Frequency Sparse Reconstruction Method

Zhongfei Ni and Binke Huang*

Abstract—The use of radar micro-Doppler (m-D) signatures for human activities classification, surveillance and healthcare has become a hot topic in recent years. While m-D signals are always multicomponent, it is necessary to separate them into mono-components signals associated with individual body parts for easier features analysis and extraction. In this paper, a novel method called local time-frequency sparse reconstruction (LTFSR) is proposed to iteratively extract and separate m-D components one by one in a descending intensity order from a time-frequency (T-F) representation. For the current strongest m-D component, we first estimate its instantaneous frequency (IF) by dividing the signal into short overlapping time intervals and selecting the best matching chirp atom to approximate the local frequency in each time interval based on matching pursuit. Then, a T-F filtering is used to extract and remove the strongest component from the multicomponent signal. Repeat the above steps until all m-D components are separated. Simulations are given to validate the effectiveness and robustness of the proposed method.

1. INTRODUCTION

Much research in recent years has been focused on sensing, classification, and recognition of human motions using radar sensors, due to many attractive attributes such as proven technology, nonobstructive illumination, nonintrusive sensing, insensitivity to lighting conditions, and privacy preservation, in competition with cameras and other sensing devices. The movement of different parts of the human body in the presence of radar illumination generates unique micro-Doppler (m-D) signature which can be extracted effectively using joint time-frequency (T-F) analysis [1, 2] and used to analyze the motion characteristics of activities.

Most existing relevant research involving human activity recognition is focused on classification and recognition of different activities such as walking, running, and jogging using machine learning (ML) techniques or deep learning based on the m-D spectrograms obtained by Short-Time Fourier Transform (STFT) [3–8]. In many applications, however, fine-grained analysis of human motion state is needed rather than recognition of different activities. For example, in application of assessing the rehabilitation state of a patient recovering from a physical injury, m-D components of interested body parts, such as arms and legs, are required to be extracted for fine-grained analysis [9, 10]. Besides, for gait-based individuals identification, it is the key to detect the minor variability in m-D signatures across individuals [11–14]. Since m-D components from different human body parts are usually overlapped in T-F domain and have large dynamic range, it is almost impossible to extract such fine-grained and very informative m-D features from linear and bilinear T-F distributions due to the limited T-F resolution and cross-term interference, which severely restrict the m-D frequencies estimation accuracy and m-D components separation.

Received 12 April 2021, Accepted 10 June 2021, Scheduled 16 June 2021

* Corresponding author: Binke Huang (bkhuang@xjtu.edu.cn).

The authors are with the School of Information and Communication Engineering, Xi'an Jiaotong University, Xi'an 710049, China.

To improve the ability of fine-grained m-D features extraction and further detail the human status identification, several human m-D components separation methods have been proposed in recent years. These methods can be divided into two classes, i.e., range-assisted separation methods and direct m-D components separation methods. Range-assisted separation method typically separates m-D components associated with different body parts in conjunction with target high-resolution range information [15–17]. The large bandwidth required to achieve high range resolution, however, will undoubtedly increase the cost of radar hardware and the complexity of processing large amounts of data. The second type of methods directly separates the m-D signals measured by low-cost Doppler radar. In [18], a modified high-order ambiguity function and CLEAN algorithm were jointly utilized to estimate and extract human m-D trajectories. However, there was no quantitative guideline for determining the order of the polynomial-phase. In [19], principal component analysis (PCA) method was utilized to decompose the whole human echo into a series of basis functions followed by a clustering process to cluster the principal components to three groups, i.e., the bulk motion, the movements of limbs except the lower legs, and the movements of lower legs and feet. This method, however, is difficult to separate multicomponent m-D signals into meaningful mono-components corresponding to physical parts of the body. The 1-D block processing algorithm was investigated in [20] to distinctly track specific limb joints. However, results showed that it was hard to clearly extract m-D signatures of upper body parts. In addition, in [21], Hilbert-Huang transform and analytical mode decomposition (HHT-AMD) was proposed to decompose multicomponent m-D signals into mono-component signals. However, since the extraction criteria of this algorithms are essentially based on echo frequency property rather than target scattering property, there can be great deviation of the extraction results from the true scattering components. Most recently, method based on Short-time fractional Fourier transform (STFrFT) and morphological component analysis (MCA) was used to separate the m-D signatures of human torso and limbs [22]. However, this method is still hard to further separate the overlapped m-D signatures of limbs.

Up to now, how to effectively separate human m-D signatures into mono-components that associate with body parts and how to estimate m-D frequencies accurately is still a challenging task. In this article, we aim to introduce a novel local time-frequency sparse reconstruction (LTFSR) method to separate multicomponent human m-D signal into mono-components associated with different body parts and to obtain accurate m-D frequencies estimation simultaneously. Exploiting the intensities difference of radar echoes from different body segments, we separate m-D components by extracting them one after another in a descending intensity order. Starting from the strongest component, we first estimate its m-D frequency by dividing the signal into short overlapping time intervals and selecting the best matching chirp atom to approximate the local frequency in each time interval based on chirp dictionary matching pursuit method, which is essentially a piece-wise linear approximation to the true instantaneous frequency (IF) trajectory. By choosing an appropriate time window length, we can get a high-precision estimation of the true m-D frequency. Then, the estimated m-D frequency is used to extract and remove the strongest component from the multicomponent signal by T-F filtering. Repeat above procedures till the energy ratio of the residual signal to the original m-D signal falls below a preselected threshold, completing the extraction and separation of all m-D components. Through this method, we can separate multiple m-D components successfully and obtain accurate m-D frequency estimation of each component simultaneously.

This paper is organized as follows. The following section gives a m-D signal model of a moving human. Section 3 describes the proposed LTFSR method to accurately estimate m-D frequencies and properly separate m-D components. Section 4 conducts a series of simulations to illustrate the validity and performance of the proposed approach. Finally, Section 5 presents the conclusion and future work.

2. SIGNAL MODEL

The composite echo from a walking human target can be expressed as the summation of echoes from multiple moving body parts of the human, such as torso, arms, and legs. For the monostatic continuous-wave (CW) Doppler radar observation scenario, the baseband echo from the human can be expressed

as

$$\begin{aligned} s(t) &= \sum_{k=1}^K \rho_k(t) \exp\left(-j\frac{4\pi R_k(t)}{\lambda}\right) + z(t) \\ &= \sum_{k=1}^K \rho_k(t) \exp(j\phi_k(t)) + z(t), \quad t \in [0, T] \end{aligned} \quad (1)$$

where K is the total number of human body parts or scattering centers; $\rho_k(t)$ and $R_k(t)$ are instantaneous amplitude and line-of-sight (LOS) range of the k -th scattering center, respectively; λ is the wavelength of the transmitted electromagnetic waves; $z(t)$ is an additive complex white noise; and T is the total observation interval.

The IF, i.e., the m-D frequency of the k -th moving body parts can be defined as

$$f_{D_k}(t) = \frac{1}{2\pi} \frac{d\phi_k(t)}{dt} = -\frac{2}{\lambda} \frac{dR_k(t)}{dt}. \quad (2)$$

Note that the superimposed signal $s(t)$ is a multicomponent and non-stationary signal composed of multiple components with different intensities due to the RCS difference of body parts. In general, the torso has the strongest scattering intensity which is much stronger than those of legs and arms.

In practical processing, the continuous-time signal $s(t)$ is first discretized with a sampling frequency F_s . The discrete-time signal is

$$s(n) = \sum_{k=1}^K \rho_k(nT_s) \exp(j\phi_k(nT_s)) + z(n), \quad n = [0, N-1] \quad (3)$$

where $T_s = 1/F_s$ is the sampling period, $z(n)$ the discrete version of complex white noise $z(t)$, and $N = \lfloor T/T_s \rfloor$ the length of signal.

3. PROPOSED METHOD

This section presents a novel local time-frequency sparse reconstruction (LTFSR) method to separate the m-D signatures. As echoes from different body parts vary in intensity, the proposed method extracts and separates m-D components one by one in a descending intensity order.

3.1. M-D Frequency Estimation

Unlike conventional IF estimation methods which first obtain a 2D joint time-frequency distribution images of signals and then extracts ridges to estimate IF laws, we propose a direct IF estimation method by sequentially selecting the best matching chirp atom in each short time window based on chirp dictionary matching pursuit to linearly approximate the real IF trajectory, as illustrated in Figure 1.

By using a sliding time window, the m-D signal can be divided into overlapping short time intervals, and the local signal over the m -th window can be approximated by a series of chirp atoms as

$$s_m(n) = \sum_{k=1}^K \rho_{k,m}(n) \exp(j\phi_{k,m}(n)) + z_m(n), \quad n = [0, N_w - 1] \quad (4)$$

where $s_m(n) = s(mL + n)$ and $z_m(n) = z(mL + n)$ are windowed signal and noise with L being the shift between two consecutive windows, and N_w is the window length.

The proposed method basically uses a chirp dictionary and selects the atoms which best match the local structure of the signal in each short time interval. Since we extract m-D components one by one and only extract the current strongest component in each iteration, the best matching chirp atom in the m -th window can be selected from the first iteration of matching pursuit algorithm [23], represented as

$$\psi_p = \arg \max_{\psi_i} \langle \mathbf{s}_m, \mathbf{\Psi} \rangle \quad (5)$$

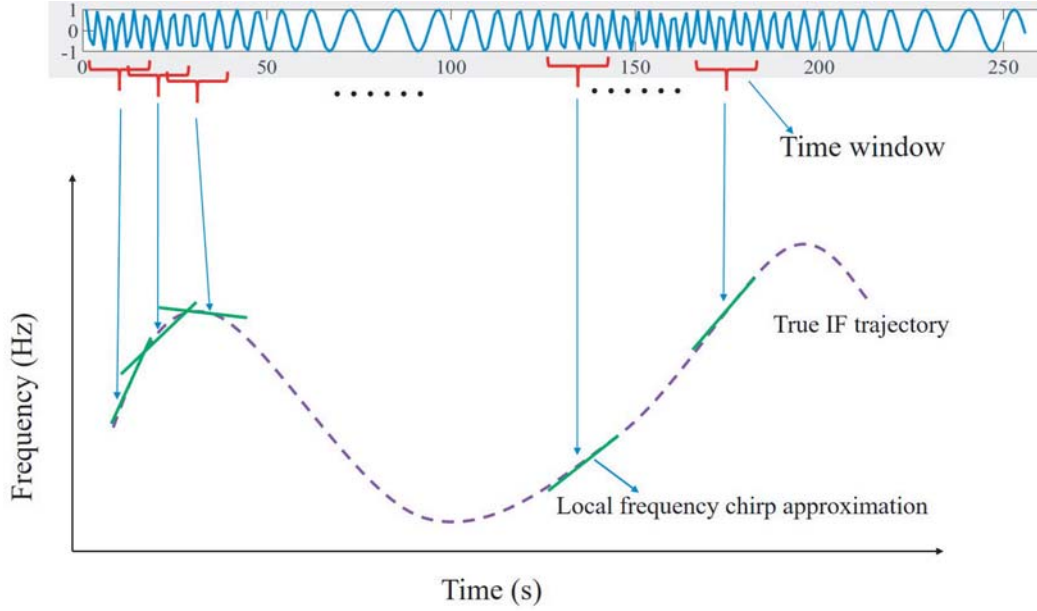


Figure 1. IF estimation using piece-wise chirp approximation.

where $\mathbf{s}_m = [s_m(0), \dots, s_m(N_w - 1)]^T$ is the signal vector over the m -th window; Ψ is the chirp dictionary that can be constructed by discretizing the 2D parameter space $\Omega = \{(\alpha, \beta) \mid |\alpha| \leq F_s/2, |\alpha + \beta T_w| \leq F_s/2\}$; ψ_m is the chirp atom that best matches the signal \mathbf{s}_m ; and $\langle \bullet, \bullet \rangle$ denotes the inner product. Specifically, the chirp dictionary $\Psi = [\psi_1, \dots, \psi_i]$, where the i -th atom $\psi_i = [\psi_i(0), \dots, \psi_i(N_w - 1)]^T$ is given by

$$\psi_i(n) = \exp\left(j2\pi\left(\alpha_i n + \frac{1}{2}\beta_i n^2\right)\right) \quad (6)$$

where α_i and β_i are the initial frequency and chirp rate.

Thus, the strongest component over the m -th window can be expressed as

$$s_{p,m}(n) \approx \rho_{p,m}(n) \exp\left(j2\pi\left(\alpha_{p,m}n + \frac{1}{2}\beta_{p,m}n^2\right)\right) \quad (7)$$

and its local frequency can be approximated by $\hat{f}_{p,m}(n) = \alpha_{p,m} + \beta_{p,m}n$. Sliding the short time window along the signal, we can accurately track and construct the entire m-D frequency trajectory sequentially. It should also be pointed out that since overlapping windows generate overlapping local linear frequency segments, a frequency averaging process is used to render unique values at each time sample.

3.2. M-D Component Extraction

Once the m-D frequency of the strongest component is estimated, it can be used to design a T-F filter [24] to extract and remove this component from the mixture m-D signal $s(t)$. Using the estimated m-D frequency $\hat{f}_p(t)$ of the strongest component, we can estimate the phase of the signal as

$$\hat{\varphi}_p(t) = \int_0^T \hat{f}_p(\tau) d\tau \quad (8)$$

which can be further used to de-chirp the strongest signal, i.e., $s_p(t) = s(t) \exp(-j\hat{\varphi}_p(t))$. When $\varphi_p(t) - \hat{\varphi}_p(t) \approx 0$, we have

$$\begin{aligned} s(t) &= \sum_{k=1}^K \rho_k(t) \exp(j\varphi_k(t)) \exp(-j\hat{\varphi}_p(t)) \\ &= \rho_p(t) + \sum_{\substack{k=1 \\ k \neq p}}^K \rho_k(t) \exp(j\varphi_k(t)) \exp(-j\hat{\varphi}_p(t)). \end{aligned} \quad (9)$$

$\rho_p(t)$ can be extracted by using a low-pass filter. Then, we can get the strongest component as

$$s_p(t) = \rho_p(t) \exp(j\hat{\varphi}_p(t)). \quad (10)$$

3.3. Summary of the Proposed Method

The main steps of the proposed LTF SR method can be summarized as follows.

- 1) Calculate the energy of the original signal $s(t)$, denoted as E_s .
- 2) Initialize the residual signal as $s_{res}(t) = s(t)$.
- 3) Estimate the m-D frequency of the strongest component in the residual signal, i.e., $\hat{f}_p(t)$, using the method described in Section 3.1.
- 4) Use the estimated m-D frequency, i.e., $\hat{f}_p(t)$, to extract the strongest component $s_p(t)$ using the T-F filtering method described in Section 3.2.
- 5) Remove the extracted signal $s_p(t)$ from the residual signal $s_{res}(t)$, i.e., $s_{res}(t) = s_{res}(t) - s_p(t)$. Then calculate the energy ratio of the residual signal $s_{res}(t)$ to the original signal $s(t)$, i.e., $\gamma = E_{res}/E_s$.
- 6) Repeat the steps from 3) to 5) till the energy ratio γ falls below a preselected threshold ξ , i.e., $\gamma < \xi$, which indicates that all m-D components are extracted and separated.

4. EXPERIMENTAL RESULTS

This section demonstrates the performance of the proposed LTF SR method to separate multicomponent m-D signatures into mono-components corresponding to different body parts. We extract m-Ds of a walking human from the motion-capture (MoCap) data available on the Carnegie Mellon University website [25], which gives a quite realistic simulations compared with the traditional Boulic model.

In simulations, each body segment is represented by a scattering point at the midpoint of two joints defining it. The human model composed of multiple scattering points walks radially from an initial relative distance of 10 m to a monostatic Doppler radar with carrier frequency 10 GHz. We interpolate the MoCap data to obtain a sampling frequency of 512 Hz. Then, radar echoes from a walking human target can be simulated. It should be mentioned that no shadowing or multiple interactions are accounted for in this model.

4.1. Estimation Accuracy of the m-D Frequency

The key to extract a m-D component from mixture signals is to estimate the m-D frequency accurately, so we first evaluate the m-D frequency estimation accuracy of the proposed LTF SR method based on chirp dictionary matching pursuit. Two m-D signals from human torso and low leg, respectively, are chosen as the interested components, because the m-D frequency of torso is approximately constant, while that of low leg shows irregular shape and dramatic variation tendency which makes it more difficult to be precisely estimated. We first give spectrograms of the two m-D signals with a 65-point Hamming window in Figs. 2(a) and (d), respectively, to clearly show the T-F characteristics.

The proposed method estimates m-D frequency by selecting the best matching atom of a chirp dictionary to approximate true IF trajectory in each short windowed slice. In simulations, we set SNR = 0 dB and use a 65-point rectangular window to slice the m-D signal with a shift step of 1 between

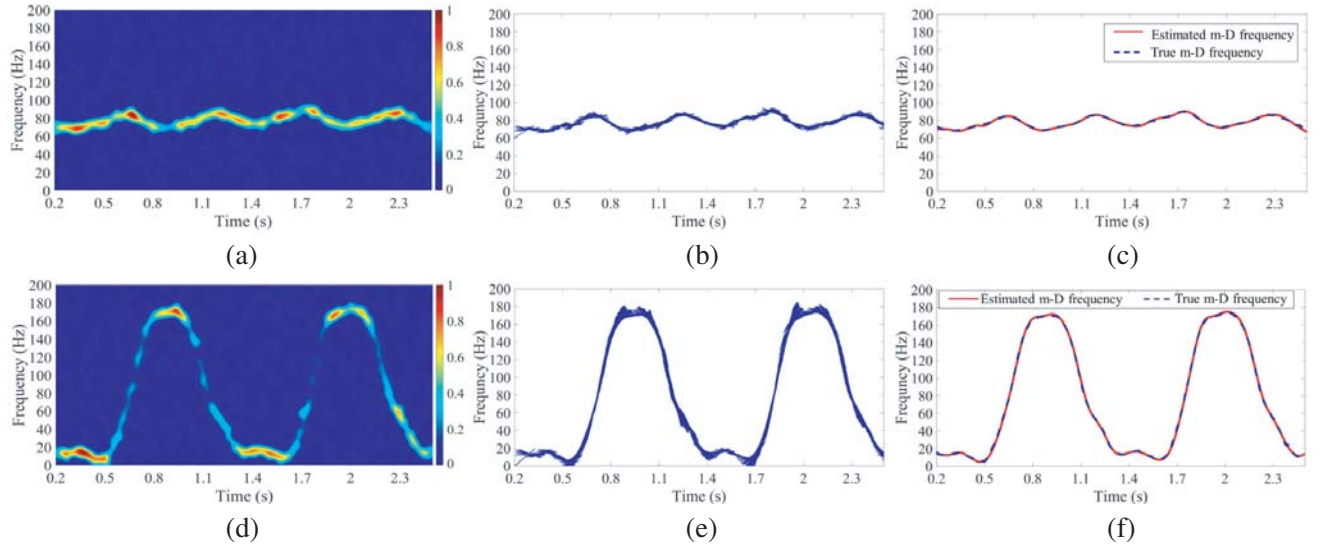


Figure 2. M-D frequency estimation based on the proposed LTF SR method (SNR = 0 dB). (a) Spectrogram of the torso m-D signal. (b) Estimated torso m-D frequency without averaging. (c) Comparison of the true and estimated torso m-D frequency with averaging. (d) Spectrogram of the low leg m-D signal. (e) Estimated low leg m-D frequency without averaging. (f) Comparison of the true and estimated low leg m-D frequency with averaging.

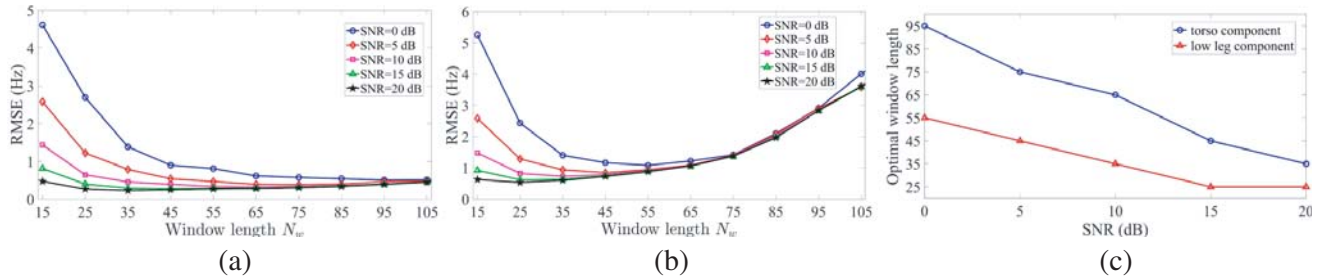


Figure 3. (a) Estimation RMSE of the torso m-D frequency against window lengths and SNRs. (b) Estimation RMSE of the low leg m-D frequency against window lengths and SNRs. (c) Optimal window lengths against SNRs.

consecutive windows. Figs. 2(b) and (c) show the constructed m-D frequencies of torso without and with averaging processing, respectively. From Fig. 2(c), one can see that the estimated m-D frequency (red solid line) agrees well with the true trajectory (blue dashed line). Results of the low leg m-D component are given in Figs. 2(e) and (f) which also clearly show the superior IF estimation capability of the proposed method, even at a relatively low SNR of 0 dB.

There are two key parameters, i.e., window length and SNR, closely related to the accuracy of m-D frequency estimation. Therefore, the root mean square error (RMSE) between the true and estimated m-D frequencies is used to quantitatively measure the accuracy of the IF estimation. Figs. 3(a) and (b) give the estimation RMSEs of torso and low leg m-D frequencies against various window lengths and SNRs, respectively, where 100 trials of Monte Carlo simulations are performed.

From Figs. 3(a) and (b), one can see that the improvement of SNR does favor the m-D estimation accuracy. Besides, the RMSE curves show a U-shape tendency as the window length increases from 15 to 105, which indicates that there is an optimal window length for each SNR. However, for the same SNR, the optimal window lengths of the two components from torso and low leg are different, by comparing Figs. 3(a) with (b). To clearly reveal the difference, we give the optimal window lengths

at different SNRs of the two m-D components in Fig. 3(c), from which we can find that the optimal window length of the low leg component is shorter than that of the torso component for the same SNR. This is reasonable. Because using a linear frequency to approximate a dramatically varied frequency may be inferior to a steadily varied one for the same window length, a balance is required in selection of the optimal window length for multicomponent signal containing various time-frequency characteristics.

4.2. Multicomponent m-D Signals Separation

M-D components from multiple moving body parts, e.g., torso and limbs, are overlapped in T-F domain and with different intensities, making it a challenge to separate these m-D signatures. In this simulation, we focus on the separation of a walking human's m-D signals into different components corresponding to the torso, left low leg, and right low arm, respectively, with an amplitude ratio of 1 : 0.35 : 0.2. Due to a similar motion status of the left low leg and the right low arm, m-D frequencies of these two parts are closely distributed and severely overlapped in T-F domain as shown in Fig. 4(a), which makes it difficult to separate the m-D components properly by traditional algorithms, such as the peak detection based on T-F imaging and the empirical mode decomposition (EMD) algorithm.

Figure 4 shows the entire separation procedures of the proposed iterative extraction method to give a more clear understanding. From the spectrogram of the multicomponent m-D signal with SNR of 15 dB shown in Fig. 4(a), one can clearly see that the component from torso is much stronger than other two components from low leg and low arm. So we first separate the m-D component from the torso.

Iteration 1: We first construct the m-D frequency trajectory of the torso component sequentially based on chirp dictionary matching pursuit using a 65-point rectangular window as a compromise to the estimation accuracy of multiple components with significantly different m-D characteristics. The estimated m-D frequency trajectories without and with averaging process are shown in Figs. 4(b) and (c), respectively. It can be seen from Fig. 4(c) that the estimated m-D frequency of the torso is in good agreement with the real trajectory. After getting the torso m-D frequency, we use T-F filtering to extract this component and remove it from original multicomponent signal.

It should be noted that the low-pass filter bandwidth is a key parameter which determines the performance of m-D component extraction and removal. When the bandwidth is too small, the detected component will not be completely extracted and removed, which will be an interference for other components. Otherwise, when the bandwidth is too large, part of other components will be extracted and removed if components are overlapped in T-F domain. A relative narrow bandwidth of 4 Hz is chosen in this simulation.

With the separation of the first strongest component, SNR of the residual signal after one iteration drops from the initial 15 dB to 7.4 dB, and the calculated energy ratio of the residual signal to the original signal is 40.6%, exceeding the preselected threshold which is set to 20% (determined by SNR). So we repeat the above procedure to separate the strongest component of the residual signal.

Iteration 2: Spectrogram of the residual signal after one iteration is shown in Fig. 4(d), and the m-D frequencies without and with averaging process of the second separated component are shown in Figs. 4(e) and (f), respectively, corresponding to the m-D component from low leg. The SNR of the residual signal after two iterations is further reduced to 3.3 dB, and the calculated energy ratio is 25.6%, still exceeding the preselected threshold, which indicates that the separation procedure should be continued. In order to see clearly, Fig. 4(g) gives the spectrogram of the residual signal after two iterations.

Iteration 3: Continuing the above separation processes, the m-D frequencies without and with averaging process of the third separated component, i.e., m-D of the right low arm, are shown in Figs. 4(h) and (i), respectively. The calculated energy ratio after three iterations is 18.9%, below the threshold, which indicates the end of iteration. Spectrogram of the residual signal after three iterations is shown in Fig. 4(j).

For now, all the three m-D components originally mixed together are extracted and separated from each other successfully. By showing m-D frequency trajectories of all components in the same picture shown as Figs. 4(k) and (l), we can get a super-resolution and more detailed m-D signatures representation than the spectrogram shown in Fig. 4(a), which will certainly offer more information for the detailed analysis of human gait.

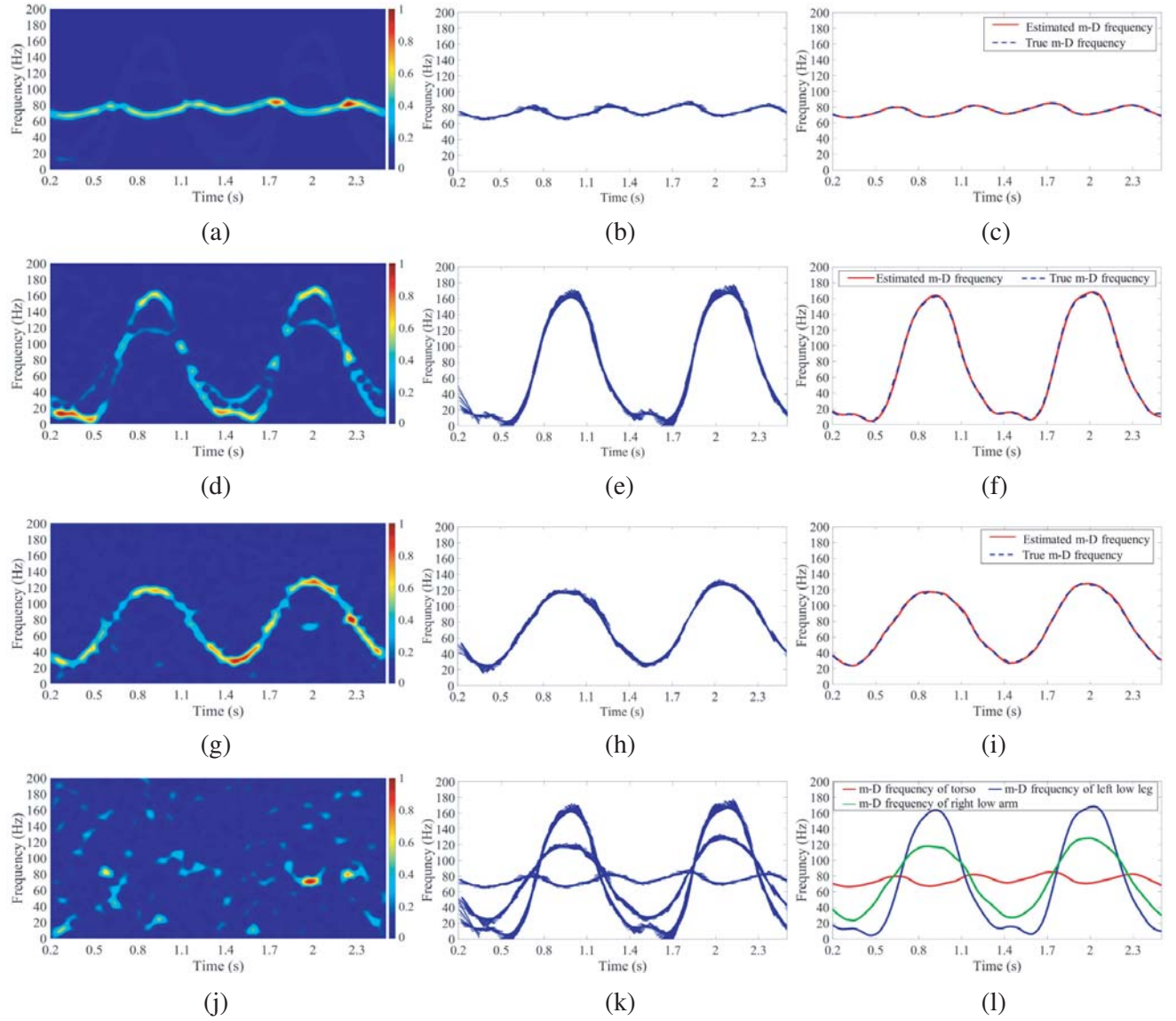


Figure 4. Walking human m-D components separation using the proposed LTFSR method. (a) Spectrogram of the original multicomponent m-D signal. (b) Separated torso m-D component without averaging. (c) Separated torso m-D component with averaging. (d) Spectrogram of the residual signal after one iteration. (e) Separated left low leg m-D component without averaging. (f) Separated left low leg m-D component with averaging. (g) Spectrogram of the residual signal after two iterations. (h) Separated right low arm m-D component without averaging. (i) Separated right low arm m-D component with averaging. (j) Spectrogram of the residual signal after three iterations. (k) All m-D frequency trajectories without averaging. (l) All m-D frequency trajectories with averaging.

Note that although our experiments did not consider the shadowing effect that can cause additional attenuation of the radar echoes, it is expected that our method can also work when we incorporate the shadowing effect because the echo intensity of the torso is definitely higher than that of each limb, and the echo intensity of the leg is also definitely higher than that of the arm, which makes it possible to separate these components based on their intensity difference. The performance validation of this method on real radar measurements with shadowing effect will be left as a future work.

5. CONCLUSION

In this article, we propose a novel local time-frequency sparse reconstruction (LTFSR) method to separate multicomponent m-D signals into mono-components associated with individual body parts in an iterative extraction manner. In each iteration, we extract the current strongest component by first estimating its instantaneous frequency based on chirp dictionary matching pursuit in short windowed T-F segments, followed by T-F filtering to separate this component. Compared with other multicomponent separation methods, such as PCA-based method, HHT-AMD, and STFrFT, our proposed method directly separates m-D components in a T-F representation, which ensures that the separated components are associated with specific physical scattering parts of the body rather than less physically meaningful descriptions, greatly facilitating the more accurate features analysis and extraction. Simulation results also show the superior separation capability of the proposed method, especially in cases of low SNR even to 0 dB. The future work will conduct a validation of the presented method on real radar measurements.

ACKNOWLEDGMENT

This research was supported in part by the National Natural Science Foundation of China (Grant No. 61471293) and the China Scholarship Council (Grant No. 201706285142).

REFERENCES

1. Chen, V. C., "Doppler signatures of radar backscattering from objects with micro-motions," *IET Signal Processing*, Vol. 2, No. 3, 291–300, 2008.
2. Narayanan, R. M. and M. Zenaldin, "Radar micro-Doppler signatures of various human activities," *IET Radar, Sonar and Navigation*, Vol. 9, No. 9, 1205–1215, 2015.
3. Kim, Y. and H. Ling, "Human activity classification based on micro-Doppler signatures using a support vector machine," *IEEE Transactions on Geoscience and Remote Sensing*, Vol. 47, No. 5, 1328–1337, 2009.
4. Ricci, R. and A. Balleri, "Recognition of humans based on radar micro-Doppler shape spectrum features," *IET Radar, Sonar and Navigation*, Vol. 9, No. 9, 1216–1223, 2015.
5. Du, H., T. Jin, Y. Song, and Y. Dai, "Unsupervised adversarial domain adaptation for micro-Doppler based human activity classification," *IEEE Geoscience and Remote Sensing Letters*, Vol. 17, No. 1, 62–66, 2019.
6. Kim, Y. and T. Moon, "Human detection and activity classification based on micro-Doppler signatures using deep convolutional neural networks," *IEEE Geoscience and Remote Sensing Letters*, Vol. 13, No. 1, 8–12, 2015.
7. Park, J., R. Javier, T. Moon, and Y. Kim, "Micro-Doppler based classification of human aquatic activities via transfer learning of convolutional neural networks," *Sensors*, Vol. 16, No. 12, 1990, 2016.
8. Li, X., Y. He, and X. Jing, "A survey of deep learning-based human activity recognition in radar," *Remote Sensing*, Vol. 11, No. 9, 1068, 2019.
9. Seifert, A.-K., A. M. Zoubir, and M. G. Amin, "Radar classification of human gait abnormality based on sum-of-harmonics analysis," *2018 IEEE Radar Conference (RadarConf18)*, 0940–0945, IEEE, 2018.
10. Seifert, A.-K., M. Amin, and A. M. Zoubir, "Toward unobtrusive in-home gait analysis based on radar micro-Doppler signatures," *IEEE Transactions on Biomedical Engineering*, Vol. 66, No. 9, 2629–2640, 2019.
11. Björklund, S., H. Petersson, and G. Hendeby, "On distinguishing between human individuals in micro-Doppler signatures," *2013 14th International Radar Symposium (IRS)*, Vol. 2, 865–870, IEEE, 2013.

12. Zenaldin, M. and R. M. Narayanan, "Features associated with radar micro-Doppler signatures of various human activities," *Radar Sensor Technology XIX; and Active and Passive Signatures VI*, Vol. 9461, 94611D, International Society for Optics and Photonics, 2015.
13. Cao, P., W. Xia, M. Ye, J. Zhang, and J. Zhou, "Radar-ID: Human identification based on radar micro-Doppler signatures using deep convolutional neural networks," *IET Radar, Sonar and Navigation*, Vol. 12, No. 7, 729–734, 2018.
14. Yang, Y., C. Hou, Y. Lang, G. Yue, Y. He, and W. Xiang, "Person identification using micro-Doppler signatures of human motions and UWB radar," *IEEE Microwave and Wireless Components Letters*, Vol. 29, No. 5, 366–368, 2019.
15. Fogle, O. R. and B. D. Rigling, "Micro-range/micro-Doppler decomposition of human radar signatures," *IEEE Transactions on Aerospace and Electronic Systems*, Vol. 48, No. 4, 3058–3072, 2012.
16. Abdulatif, S., F. Aziz, B. Kleiner, and U. Schneider, "Real-time capable micro-Doppler signature decomposition of walking human limbs," *2017 IEEE Radar Conference (RadarConf)*, 1093–1098, IEEE, 2017.
17. He, Y., P. Molchanov, T. Sakamoto, P. Aubry, F. Le Chevalier, and A. Yarovoy, "Range-Doppler surface: A tool to analyse human target in ultra-wideband radar," *IET Radar, Sonar and Navigation*, Vol. 9, No. 9, 1240–1250, 2015.
18. Ding, Y. and J. Tang, "Micro-Doppler trajectory estimation of pedestrians using a continuous-wave radar," *IEEE Transactions on Geoscience and Remote Sensing*, Vol. 52, No. 9, 5807–5819, 2014.
19. Shi, X., F. Zhou, M. Tao, and Z. Zhang, "Human movements separation based on principal component analysis," *IEEE Sensors Journal*, Vol. 16, No. 7, 2017–2027, 2015.
20. Quaiyum, F., N. Tran, J. E. Piou, O. Kilic, and A. E. Fathy, "Noncontact human gait analysis and limb joint tracking using Doppler radar," *IEEE Journal of Electromagnetics, RF and Microwaves in Medicine and Biology*, Vol. 3, No. 1, 61–70, 2018.
21. Li, W., G. Kuang, and B. Xiong, "Decomposition of multicomponent micro-Doppler signals based on HHT-AMD," *Applied Sciences*, Vol. 8, No. 10, 1801, 2018.
22. Qiao, X., T. Shan, R. Tao, X. Bai, and J. Zhao, "Separation of human micro-Doppler signals based on short-time fractional fourier transform," *IEEE Sensors Journal*, Vol. 19, No. 24, 12205–12216, 2019.
23. Mallat, S. G. and Z. Zhang, "Matching pursuits with time-frequency dictionaries," *IEEE Transactions on Signal Processing*, Vol. 41, No. 12, 3397–3415, 1993.
24. Zhang, H., L. Yu, and G.-S. Xia, "Iterative time-frequency filtering of sinusoidal signals with updated frequency estimation," *IEEE Signal Processing Letters*, Vol. 23, No. 1, 139–143, 2015.
25. Shell, M., "Carnegie mellon university motion capture database," 2012.